Journal of Techniques, ISSN: 2708-8383, Vol. 8, No. 1, 2026, Pages 107-117
https://doi.org/10.51173/jt.v8i1.2809

JOURNAL OF TECHNIQUES

Journal homepage: http://journal.mtu.edu.iq

RESEARCH ARTICLE - MECHANICAL ENGINEERING

Numerical Investigation on the Effect of Using a Heat Sink Integrated with Nano-PCM on the PV Cell Temperature

Hussian A. Abdul Kareem[1*], Anwar S. Barrak[2], Oula M. H. Fatla[3]

[1]Engineering Technical College - Baghdad, Middle Technical University, Baghdad, Iraq

[2]Imam Ja'afar Al-Sadiq University, Baghdad, Iraq

[3]Mechanical Engineering Department, College of Engineering, Gulf University, Sanad, Kingdom of Bahrain

[*] Corresponding author E-mail: huseinali@mtu.edu.iq

Article Info.

Article history:

Received
11 January 2026

Revised
09 March 2026

Accepted
17 March 2026

Published
31 March 2026

Abstract

This work is a simulation study of cooling feasibility for a 570 x 670 mm solar cell rated at 50 W, evaluated using COMSOL Multiphysics 6.1. Specifically, the effect of the number of flat fins on the cell temperature is examined. To determine the optimal number of fins, the impact of three fin cross-sections—flat, triangular, and T-shaped—is investigated. Following the selection of the optimum cross-section, the effect of adding a nano-PCM mass to the heat sink is studied. Several masses are analyzed by varying the height of the nano-PCM mass container, with dimensions of 20, 30, and 40 mm. Once the optimum tank height is identified, the feasibility of using water to cool the nano-PCM mass is assessed. The results indicated that eight flat fins can yield a similar temperature despite that the lowest cell temperature has been achieved with 10 flat fins. Therefore, the number of fins is fixed at 8, which reduces the cell temperature to 52.6 °C, a 10% improvement. Subsequently, using triangular-section fins instead of flat ones can reduce the maximum temperature to 50.8 °C, representing an 11.8% improvement. Supporting the heatsink with a 40 mm-thick container filled with nano-PCM can further reduce the cell temperature to 44.67 °C (by 22.5%). Finally, the lowest maximum cell temperature is obtained as 37.9 °C when the nano-PCM described above is cooled with water, resulting in a 34.1% improvement.

Publisher: Middle Technical University

Keywords: CFD Simulation; FEM; Cooling PV; PV Cell; Nano-PCM; Fins Geometry.

1. Introduction

The exploitation and use of non-renewable resources have consistently marred human existence and progress. To achieve sustainable resource exploitation and foster harmonious coexistence between human beings and nature, the world is actively promoting new energy [1] by introducing sustainable energy as a clean, renewable alternative, such as solar, which is the most promising. Solar Photovoltaic (PV) is the conversion of solar irradiance into electrical power. PV has several advantages, including minimal maintenance, no moving parts in operation, a non-polluting operating process, and a long service life. However, the main obstacle has been their low conversion efficiency, typically 5-20% of incident solar irradiance [2, 3]. Currently, a solar technology that integrates solar thermal collectors with PV modules into a single unit, known as a photovoltaic/thermal (PV/T) system, is being developed [4, 5].

A study by Jiang et al. [5] found that fractal fins can reduce the cell temperature of a photovoltaic panel by 2 °C relative to regular fins. The optimal configuration was a 120 × 50 mm cavity with a PCM thickness of 40 mm. With a second fin, the temperature was reduced by an additional 2.3 °C. This indicates that the combination of PCM and fin design is crucial for thermal management in PV systems. Khelifa et al. [6] investigated a SPVT system with skin-tube-like fins. They reported an effective daily yield of 2.02 kWh, which is 55.1% higher than that of conventional systems. Hong et al. [7] studied T-shaped fin arrays in a PCM heat sink. These fins enhanced temperature uniformity by predominantly disrupting natural convection during melting. The melting time was reduced by 25.5% for T-shaped fins, compared to the un-fined system, and by 14.5% compared to rectangular fins. The two pilot plants also reduced wall temperature by 18.9 °C and 4.9 °C, respectively. The results ascertained that T-shaped fins effectively enhance the heat-sink performance of PCM. Khelifa et al. [8] investigated finned photovoltaic solar collectors across three cases: no fins, 20 fins, and 40 fins. They discovered that thermal efficiency increased with the number of fins and with solar radiation but declined slightly with increasing water flow rate. At a flow rate of 0.01 kg/s, the thermal efficiencies were 50.54%, 52.33%, and 54.25%, respectively. The third cooling-and-energy-gain configuration yielded the best results.

Alqatamin et al. [9] designed a heatsink with perforated wave-shaped fins to maximize photovoltaic cell performance. Their simulations showed that the PV-PWSF system reduced panel temperature to 57.8 °C under 1000 W/m² irradiance. Efficiency increased to 12.79%. Power output also rose to 15.6%. The temperature dropped further to 47.7 °C at an airflow velocity of 2.5 m/s. This is much lower than the ambient air

Nomenclature & Symbols			
c_p	Specific Heat Capacity (J/kg K)	U	Velocity in X-Direction (m/s)
d	Diameter (cm)	V	Velocity in Y-Direction (m/s)
g	Gravity (m/s^2)	W	Velocity in Z-Direction (m/s)
G	Solar Radiation (W/m^2)	∂x	Elements in the X-Direction (m)
h	Heat Transfer Coefficient (W/m^2·K)	∂y	Elements in the Y-Direction (m)
k	Thermal Conductivity of Material (W/m K)	∂z	Elements in the Z-Direction (m)
L	Length (cm)	μ	Dynamic Viscosity Pa · s
L_f	Latent Heat (kJ/kg)	ρ	Density kg/m^3
m°	Mass Flow Rate (kg/s)	PV	Photovoltaic
p	Pressure (Pa)	PCM	Phase Change Material
Q_{in}	Heat Source (W/m^3)	Nano-PCM	Nanoparticles- Phase Change Material
T	Temperature (℃)	CFD	Computational Fluid Dynamics
t	Time (s)	FEM	Finite Element Method

temperature. Thus, wind isolation could effectively cool the PV system and alleviate hotspots. The design used frequent waves of 10 cm wavelength and about 1.5 cm height. Bashir and Ali [10] analyzed passive cooling of PV modules using extended-fin heat sinks. They identified design factors to maximize efficiency. For a 50 W solar panel, they found that heat loss increased linearly with fin length. It also rose sharply with fin diameter between 8 and 12 mm. Heat loss was higher at high temperatures and with many fins. With rectangular pin fins, heat losses increased by 33.77% compared to circular fins. Losses rose by 41.4% compared to long rectangular fins. Du et al. [11] studied Cantor fractal fin arrays in a photovoltaic-phase change material (PV-PCM) system. These fins improved temperature uniformity and heat transfer. Wall temperature decreased by at least 9.1 °C. Cantor fins performed better than rectangular fins. PCM uniformity and efficiency improved with transverse flow. However, wall-temperature uniformity decreased. These results showed that Cantor fins could be ideal for thermal management in solar collectors. Unnikrishnan et al. [12] tested and simulated a PV-PCM system with wavy fins at 0°, 15°, and 30° inclinations under 750 W/m². They demonstrated that inclination improved thermal performance. Temperature reductions were greater with up to 5 fins: 30.1 °C for PV-PCM and 38.6 °C for finned PV-PCM, compared to regular PV systems. H increased from 28.15% to 22.27% at 0° and 30°, respectively.

Pu et al. [13] investigated the thermal behavior of PV panels with PCM heat sinks equipped with T-shaped fins. A 180° T-shaped fin reduced the PV cell temperature by 15.1 K and improved electrical efficiency by 1.36%. Efficient heat transfer increased by 1.40%. Temperature uniformity was enhanced by 71.0%. Another fin arrangement was found unacceptable for effective cooling. These results demonstrated the benefits of the T-shaped fins for solar panel performance. Abdel Salam et al. [14] examined fin design in photovoltaic thermal systems. They found that electrical and thermal performance efficiencies for a 9 mm fin are 15.982% and 0.82, respectively. The peak merit function was 2.829 with a fin, compared to 2.473 for a finless design. This signified that a fin on the sensing element offered substantial gains.

Al-Omari et al. [15] studied heat sinks that use PCM, which absorbs and releases heat at certain temperatures by changing between solid and liquid. They tested different fin shapes to improve heat transfer from the source. Fins attached directly to the heat sink held less PCM, while detached fins allowed for more PCM storage. Even when both types had the same surface area, attached fins still contained less PCM. Making the heat sink wider and taller helped the PCM lower peak temperatures more effectively because the larger surface area allowed for better heat dissipation. These results provide useful advice for designing more efficient heat sinks. Madhi et al. [16] looked at how fin angle affects cooling in PV/T systems, which generate both electricity and heat from solar energy. They found that a 30° fin angle gave the best heat transfer, while a 90° fin had the highest total heat transfer. The system's electrical efficiency improved by 0.8% to 1.5%, and thermal efficiency increased to 59%.

Ambreen and Kim [17] found that circular fins filled with nanofluid provided the best cooling performance. Nanofluid, a liquid containing tiny particles suspended in it, helps transfer heat more efficiently. Hexagonal and square fins did not work as well, and water-cooled square fins performed the worst. Circular fins helped airflow more evenly, improving cooling. Placing fins near the leading edge also made a big difference, showing that both the shape and position of fins matter. Bayrak et al. [18] studied how fin design affects the temperature and output of air-cooled solar panels. They found that a 7 by 20 cm interlaced fin setup worked best, yielding 11.55% power output and an exergy factor of 10.91%, indicating how well energy is converted into useful work. Ghanim and Farhan [19] found that zigzag surfaces performed best at low airflow rates (below 0.06 kg/s), while regular fins performed better at higher airflow rates. Using both methods together increased thermal efficiency by 3% and electrical efficiency by 26%. Kim and Nam [20] used computer models to study solar panel cooling. Without additional cooling, the panel reached 62.78 °C and had an efficiency of 14%. Adding fins lowered the temperature by 15.13 °C and raised efficiency to 14.39%. Adding slits between fins further improved airflow, dropping the temperature by another 8.62 °C at lower airflow rates while keeping the panel temperature steady. This stability helped improve efficiency and made the panel work more reliably. The study highlighted several good ways to cool solar panels. Mustafa et al. [21] used 3D computer models and found that circular pin fins kept solar panels coolest. Triangular pin fins made the panels hottest. They also caused the largest melting in the PCM. D. Kameswara Rao et al. [22] studied both experimentally and theoretically the use of CPCM combined with fins for cooling solar PV panels. The results showed that adding CPCM with a heat sink reduced the panel temperature by up to 13.9 °C compared with the reference panel.

This study used COMSOL Multiphysics 6.1 to identify cooling strategies for a 570 x 670 mm PV cell and to improve the combined PV/T system efficiency. It tested various flat-fin configurations to find the best options. The study also looked at how different amounts of nano-PCM and cooling the nano-PCM with water affected PV cell performance.

2. Numerical Method

2.1. Physical model

Numerical simulations of cooling PV modules by different methods were carried out using COMSOL Multiphysics 6.1. The study simulated a PV/nano-PCM system to improve heat control and electrical efficiency. The system contained a typical polycrystalline silicon PV module, a nano-PCM box with a water pipe, and an aluminum heat sink. The main equations were solved with the finite element method (FEM).

Several important factors influence the thermal and electrical performance of the PV/nano-PCM cooling system. These include geometric conditions, the number and arrangement of fins, fin shape, the height of the nano PCM container, the type of PCM (with or without nanoparticles), and whether an inserted water pipe is present. The four primary variables analyzed were: (i) number of fins, (ii) fin configuration, (iii) Nano PCM container height, and (iv) water pipe insertion. The ranges and selected levels for these variables are summarized as follows:

- Number of fins: 8, 10, and 12 fins
- Fin configuration: flat, T-shaped, and triangular-shaped geometries attached to the bottom surface of the PV panel
- The height of the nano PCM container was 2, 3, and 4 cm (with increments of 1 cm).

Fig. 1 shows the physical dimensions of the PV/nano PCM system. Fig. 2 illustrates the ship-of-fins study, the design methods, and the geometric parameters of the fins. Tables 1 to 3 provide details on the thermo-physical properties of the PV layer, the nano-PCM, and the fins.

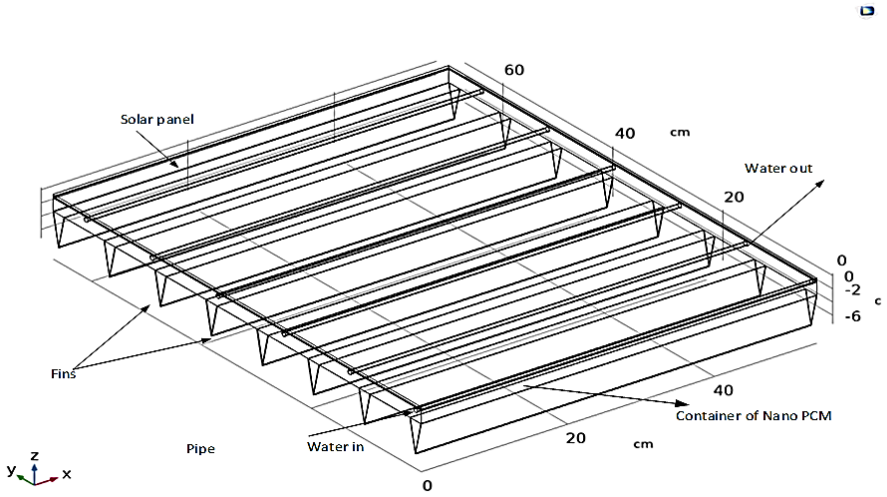

Fig. 1. Schematic diagram of the PV nano PCM system

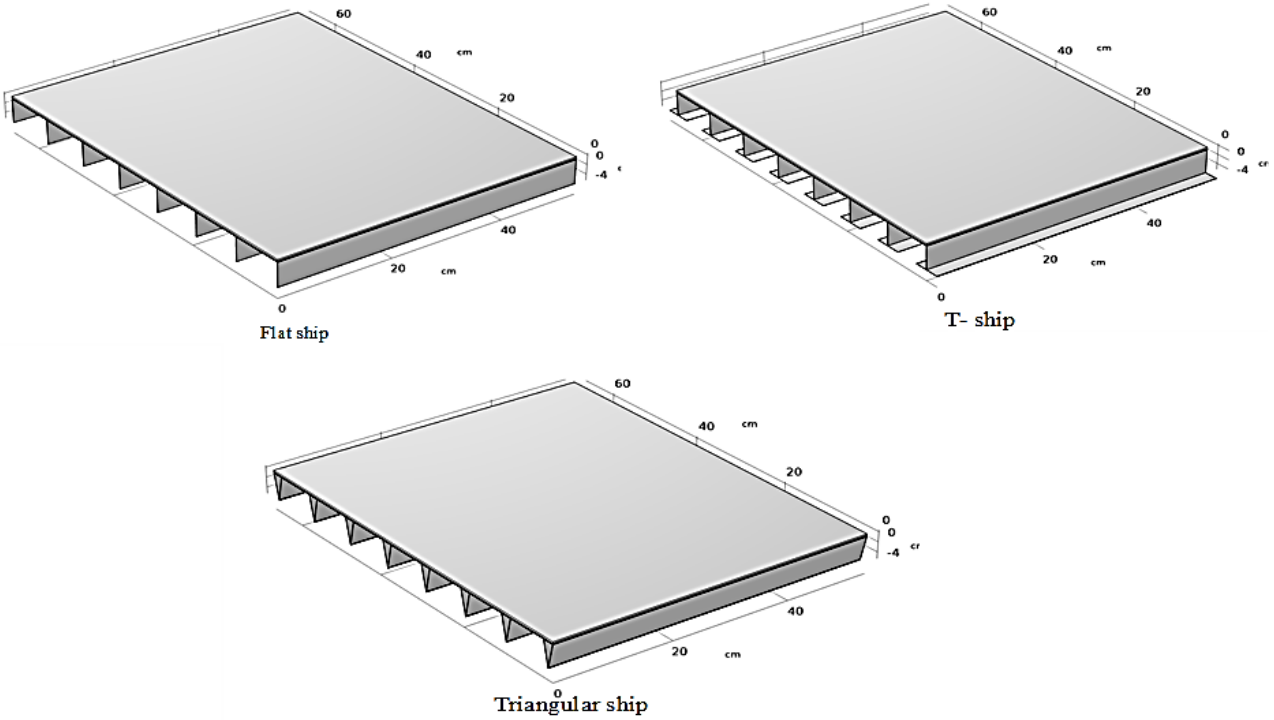

Fig. 2. Ship of fins study

Table 1. Thermophysical properties of PV panel and PMD layers [23]

No	Material	Thermal conductivity (W/m K)	Density(kg/m^3)	Specific heat (J/kg K)
1	Water	0.625	991	4172
3	Silicon	148	2330	677
4	EVA	0.35	960	2090
5	Glass	1.8	3000	500
6	Tedlar	0.2	1200	1250
7	Aluminum	238	2700	900

Table 2. Characteristics of Al2O3 nanoparticles [24]

Property	Nano PCM
Density (kg/m³)	3600
Specific heat (J/kg K)	765
Thermal conductivity (W/m K)	36
Viscosity (N.s/m^2)	$\mu = 0.001e^{-4.25+\frac{1790}{T}}$
Heat of latent (kJ/kg)	$L_f = 160$
Temperature of Melting (°C)	56

Table 3. Dimensions of the main parts of the PV/nano PCM model

Dimension	Value (cm)
Solar cell	67*54*0.5
Container of PV/nano PCM	67*54*(2, 3,4)
Height of fins	5
Number fins	6, 8, and 10
Length and diameter of the pipe	L=54, d=0.7
Flow rate	0.002775 [kg/s]
Temperature of inlet water	25 ℃

2.2. Governing equations

The conservation equations for mass, momentum, and energy form the foundation of the governing equations used to determine the distributions of velocity, pressure, and temperature within the computational domain of the PV/nano PCM simulation model. These equations can be expressed as follows [25-27]:

- Continuity equation:

$$\frac{\partial \rho}{\partial t} + \left(\frac{\partial \rho u}{\partial x} + \frac{\partial \rho v}{\partial y} + \frac{\partial \rho w}{\partial z}\right) = 0 \quad (1)$$

- Momentum equation:

$$\rho \frac{\partial u}{\partial t} + \rho(u\frac{\partial u}{\partial x} + u\frac{\partial v}{\partial y} + u\frac{\partial w}{\partial z}) = \mu(\frac{\partial^2 u}{\partial x^2} + \frac{\partial^2 u}{\partial y^2} + \frac{\partial^2 u}{\partial z^2}) + \rho g - \frac{\partial P}{\partial x} \quad (2)$$

$$\rho \frac{dv}{dt} + \rho\left(v\frac{\partial u}{\partial x} + v\frac{\partial v}{\partial y} + v\frac{\partial w}{\partial z}\right) = \mu\,(\frac{\partial^2 v}{\partial x^2} + \frac{\partial^2 v}{\partial y^2} + \frac{\partial^2 v}{\partial z^2}) + \rho g - \frac{\partial P}{\partial y} \quad (3)$$

$$\rho \frac{\partial w}{\partial t} + \rho(w\frac{\partial u}{\partial x} + w\frac{\partial v}{\partial y} + w\frac{\partial w}{\partial z}) = \mu(\frac{\partial^2 w}{\partial x^2} + \frac{\partial^2 w}{\partial y^2} + \frac{\partial^2 w}{\partial z^2}) + \rho g - \frac{\partial P}{\partial z} \quad (4)$$

- Energy equation [28, 29]:

For fluid flow and solar PV panels.

$$\rho\, C_P\, \frac{\partial T}{\partial t} + \rho\, C_p\left(u\, \frac{\partial T}{\partial x} + v\, \frac{\partial T}{\partial y} + w\, \frac{\partial T}{\partial z}\right) = k\, \left(\frac{\partial^2 T}{\partial x^2} + \frac{\partial^2 T}{\partial y^2} + \frac{\partial^2 (T)}{\partial z^2}\right) + Q_{IN} \quad (5)$$

$$\frac{\partial^2 T}{\partial x^2} + \frac{\partial^2 T}{\partial y^2} + \frac{\partial^2 T}{\partial z^2} = \frac{\rho Cp}{k}\frac{\partial T}{\partial t} \quad (6)$$

2.3. Assumptions

The following basic assumptions were adopted by developing the simulation model:

- Incompressible, laminar flow of fluid through the pipe channels; switching was steady and predictable.
- The thermal resistance across the different layers of the stack was not considered to simplify its calculation.
- Unsteady-state problem and 3D heat transfer in the computational domain.
- The fluid's thermophysical properties were dynamically temperature-dependent, introducing a realistic element to the simulations.
- Environmental temperatures and solar energy levels are considered time-varying to be more realistic.

2.4. Initial and boundary conditions

These considered assumptions formed the backbone of the simulation, setting the stage for insightful and impactful results. Based on the computational domain shown in Fig. 3, the initial and boundary conditions for fluid and solid walls were as follows:

2.4.1. Fluid Flow

- Inlet Conditions: The analysis began by setting the inlet parameters. Vin, Tin, ρin, and Cp for water were used as the starting point, forming the basis for the fluid dynamics study.
- Outlet Condition: The outlet pressure was measured at the water's exit point to clearly show the flow's final state.

2.4.2. Solid Surface (Walls)

- No-Slip Condition: The fluid touching the solid walls was set to have zero velocity (u = 0, v = 0, w = 0). This keeps the interaction between the fluid and the surfaces stable.
- Thermal Continuity: The temperature at the wall did not change suddenly, so heat could transfer smoothly.
- Adiabatic Surfaces: For insulated surfaces, an adiabatic condition was used. This means no heat transfer happens (q = 0 or dq = 0), so energy remains in the system.

2.4.3. Solar PV Panel:

- The top surface of the PV panel is exposed to outdoor conditions, where it receives solar radiation (G, measured in W/m²) and converts it into useful power.
- Heat leaves the top surface of the panel through both convection and radiation.
- An Aluminum sheet attached to the back of the solar PV panel acts as a heat sink. It helps manage heat by staying in direct contact with the panel's rear surface.
- This description shows how fluid flow and heat transfer work in solar PV panels, highlighting their role in making solar energy use more efficient.

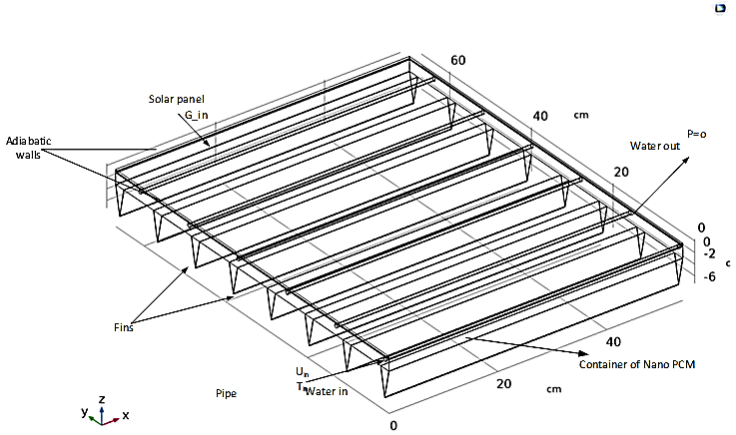

Fig. 3. Boundary conditions of the PV/PCM model computational domain

2.5. Mesh and time step independent study

Fig. 4 shows how the surface temperature changes for different grid elements over several time intervals, which helps assess the impact of grid number and time step. To balance accuracy and computational cost, we used 752030 grid points and an adaptive time step, starting at 0.001. Also checked that the solution converged by setting the relative tolerance to 10^{-6}.

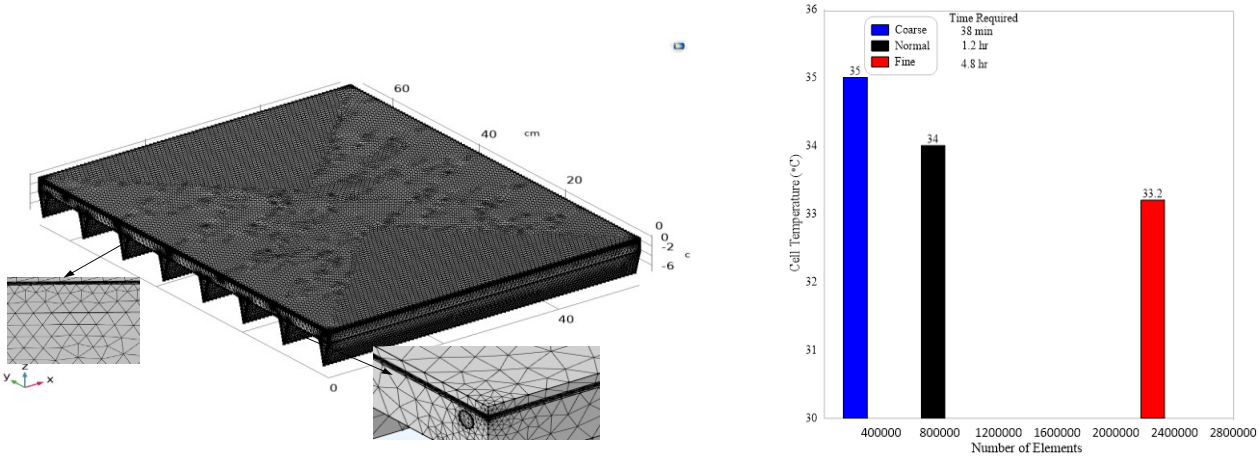

Fig. 4. Mesh independent of PV/nano PCM system

3. Results and Discussion

The theoretical simulations used the typical climate conditions of Baghdad, Iraq (33.3152° N, 44.3661° E). Fig. 5 shows that the meteorological data came from METEONORM 8 (Global Weather Data, Version 8), a reliable and comprehensive source for this analysis.

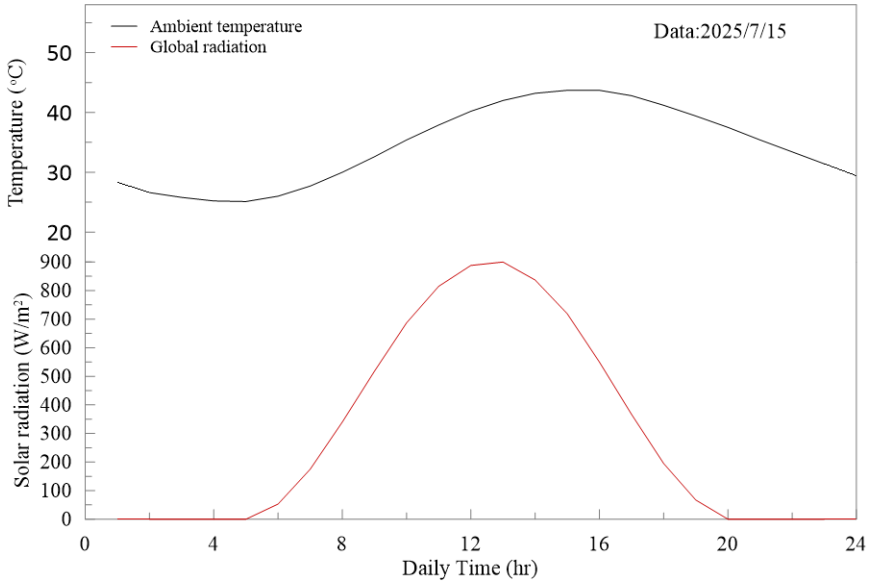

Fig. 5. Weather data for Baghdad, Iraq (33.3152° N, 44.3661° E) in July 2025

The cooling performance of the solar panel PV system was tested in four scenarios. These included changes in the number of fins, how the fins were arranged, the height of the PCM container, and whether a water pipe was used.

The heat sink helped the PV module perform better by removing excess heat, reducing the problems caused by high temperatures. The best cooling happened when stored heat travelled through the fin base and was released by convection. Good thermal conductivity made heat transfer more efficient, and adding fins increased the surface area, which improved heat rejection. As shown in Fig. 6, increasing the number of fins further lowered the peak temperature. Fig. 6 shows that the cell's highest temperature occurred around 13 hr due to PV panel heat storage. Specifically, the highest temperature was approximately 57.5 °C for the PV without fins. After adding six fins, the temperature decreased to 53.7 °C (a 6.6% reduction). With eight fins, the temperature further decreased to 52.6 °C (an 8.5% reduction). The largest reduction was with 10 fins, lowering the temperature to 51.7 °C (a 10% reduction).

Fig. 7 shows the temperature contours for the heat sinks. As illustrated, the distribution of heat depends on the number of fins, with heat concentrating in the center of the sink. This occurs because heat is easily transferred from the edges by convection. Accordingly, increasing the number of fins improved heat dissipation efficiency in the sink's center. However, despite this improvement, the center remained the hottest area.

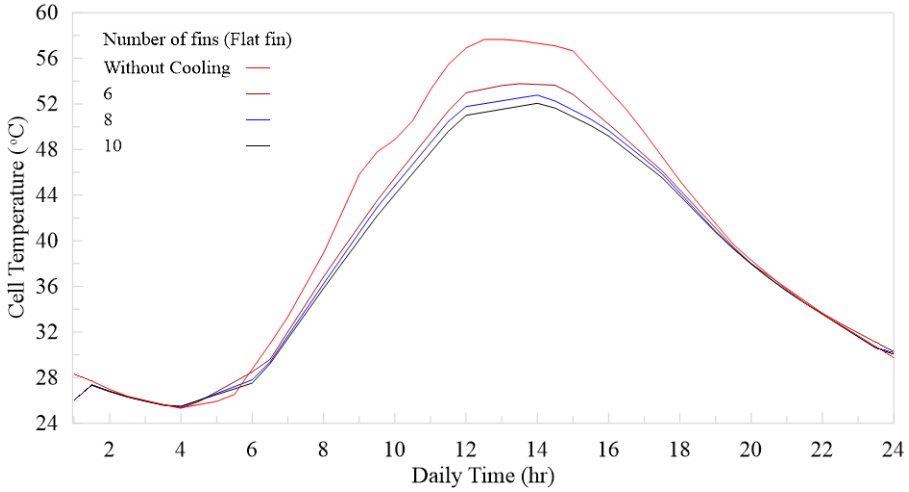

Fig. 6. Influence of the number of fins on cell surface temperature

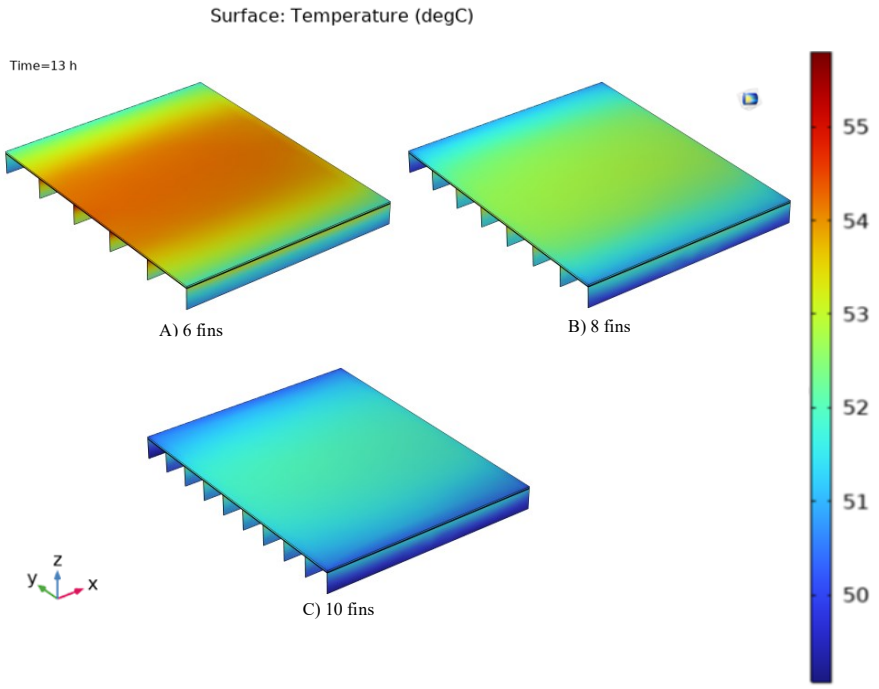

Fig. 7. Illustrates the distribution of temperature contours for varying numbers of fins

Three fin configurations were considered: flat, T-shaped, and triangular, each used separately to cool the PV panel. Fig. 8 shows how different fin shapes affect the thermal performance of the PV cell. For a fair comparison, each setup used eight fins. According to Fig. 8, triangular fins kept the cell coolest, dropping the maximum temperature from 57.6 °C (bare panel) to 50.8 °C at 2:00 PM, which is an 11.11% improvement. The T-shaped fin lowered the temperature to 51.75 ± 8 °C at 2:00 PM, a 10.25% reduction. The flat fin reached 52 °C at 2:00 PM, giving an 8.4% improvement.

Fig. 9 displays temperature contours for the PV cell employing various fin cross-sections. The flat fin exhibited Fig. 9 shows temperature contours for the PV cell with different fin shapes. The flat fin had the highest temperature, followed by the T-shaped fin, while the triangular fin worked best for cooling. The plate edges were the coolest because of heat loss from the fin surfaces. The triangular fin performed best because its thick base improved heat transfer, its tapered shape helped spread heat and lower resistance, and the upper part offered a large convective area for its weight. Additionally, it was lightweight, cost-effective, and required less material. After selecting the optimal fin geometry and number, a 20 mm nano-PCM container was placed between the heat sink and the PV cell's back.

Fig. 10 compares three scenarios: (1) a cell without fins, (2) a cell with 8 fins, and (3) a cell with 8 fins and nano-PCM placed between the cell and the heat sink. A significant decrease in cell temperature was observed upon adding nano-PCM. The shift in maximum temperature occurred toward the afternoon by about 3 hours relative to the uncooled cell and by about 1 hr relative to the finned cell. The maximum cell temperature dropped to about 44.675 °C with nano-PCM, compared to 57.66 °C without cooling. Cooling the cell using fins reduced the temperature by approximately 11.8%, while adding nano-PCM to the fins raised this reduction to 22.5%. After 18 o'clock, Fig. 10 shows that the cell temperature with nano-PCM becomes higher than that without cooling, due to latent heat storage within the nano-PCM.

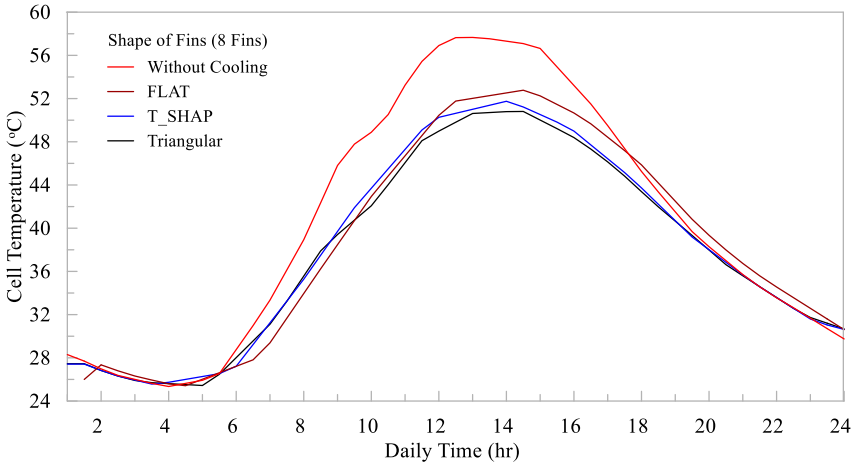

Fig. 8. Configuration of fins in the bottom panel affects the solar panel surface temperature

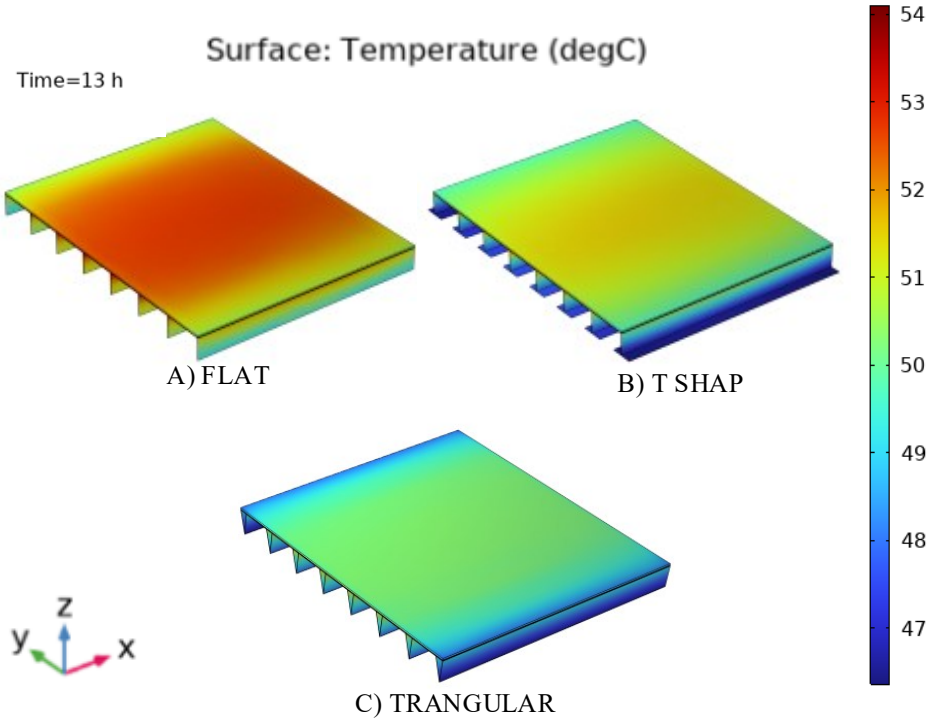

Fig. 9. Distribution of temperature contours for shape configurations of fins

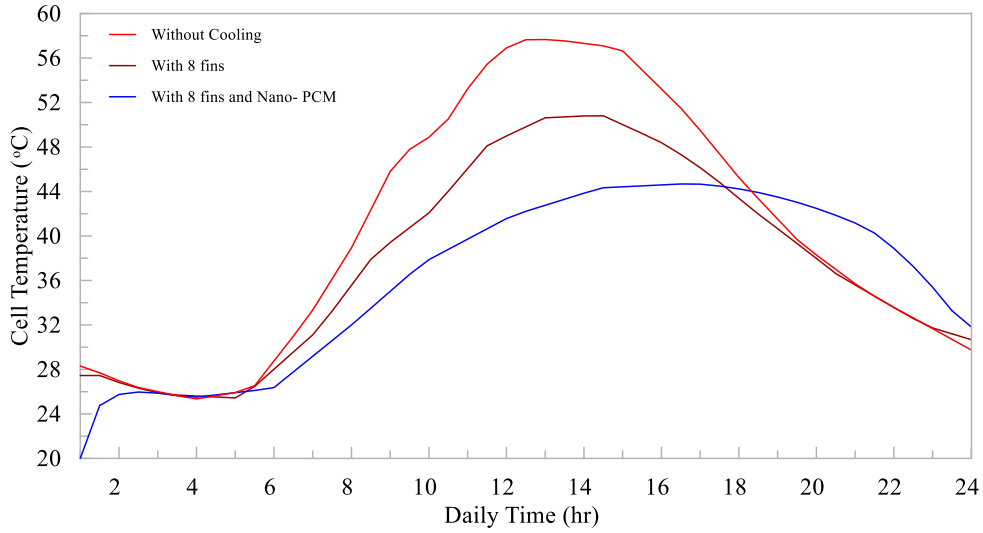

Fig. 10. Effect of nano-PCM integration on PV cell temperature

To select the best nano-PCM container thickness, three options—20, 30, and 40 mm—were evaluated to increase mass and improve cell temperature stability. As shown in Fig. 11, greater container thickness led to lower cell temperatures due to greater mass and increased heat absorption during the day. After sunset, the thickest container showed the highest cell temperature because it stored more latent heat of fusion. The lowest cell temperature, 44.67 °C, occurred in the 40 mm container. Compared to an uncooled cell, the temperature was reduced by 19.3% for 20 mm, 21.7% for 30 mm, and 22.5% for 40 mm.

Fig. 12 shows the contour plot of the phase transition between the solid and liquid phases for a 40 mm-thick nano-PCM container. The solidification percentage of the nano-PCM was approximately 84% at 13 o'clock. As nano-PCM heat absorption increases, the solidification percentage drops to 69%. This explains the decrease in cell temperature at 15 o'clock, as shown in Fig. 12. After this time, some nano-PCM remained liquid at 19 o'clock, resulting in a higher temperature in the nano-PCM-supported cell than in the cell without cooling.

To assist in removing heat generated in the cell and transferred to the nano-PCM, and prevent any additional increase in its operating temperature, the possibility of cooling the nano-PCM with water was investigated by immersing copper tubes within the nano-PCM container. Water circulated through these tubes to remove heat at a fixed flow rate of 28 kg/m² h. A network of 7 mm copper tubes, 54 cm long, was used to circulate cooling water from 8 to 20 o'clock, as shown in Fig. 13. Fig. 13 shows a significant decrease in cell temperature when the nano-PCM was cooled with water. The highest daytime cell temperature was recorded at 2:00 PM, reaching 35.5 °C. When the water flow stopped at 20 o'clock, the cell temperature increased to 38 °C due to the continuously molten PCM. The following morning, the nano-PCM cell's temperature without cooling was similar to that of the cooled cell. Fig. 14 compares results with the cell without cooling. All cases had eight

fins of triangular cross-section. One case used only the heat sink with 8 fins; another used nano-PCM with the fins; and the last combined 8 fins, nano-PCM, and water cooling from 8:00 AM to 18:00. The best-case scenario was the use of 8 triangular-section fins with nano-PCM and water cooling, showing a maximum daytime temperature of approximately 35.7 °C, which is lower than the ambient temperature of 43.7 °C and reflects a 34.1% improvement over the bare cell. This was followed by the heat sink with 8 fins and nano-PCM, reaching 44.7 °C and a 22.5% improvement, whereas using only the heat sink with fins resulted in a cell temperature of 50.8 °C and an improvement of 11.9%.

The results are compared against those of D. Kameswara Rao [22], as shown in Fig. 15. The comparison shows an 18% deviation in cell temperature and a 24% deviation in the temperature difference between the cell and ambient temperatures.

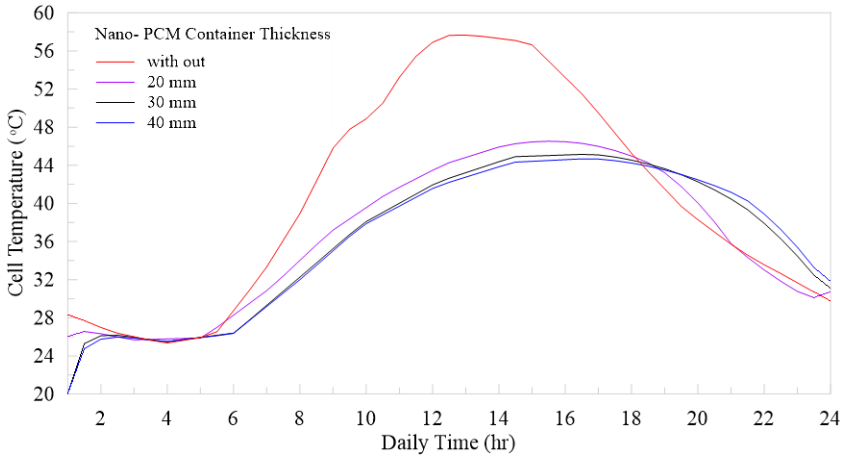

Fig. 11. Effect of nano-container height on the cell temperature

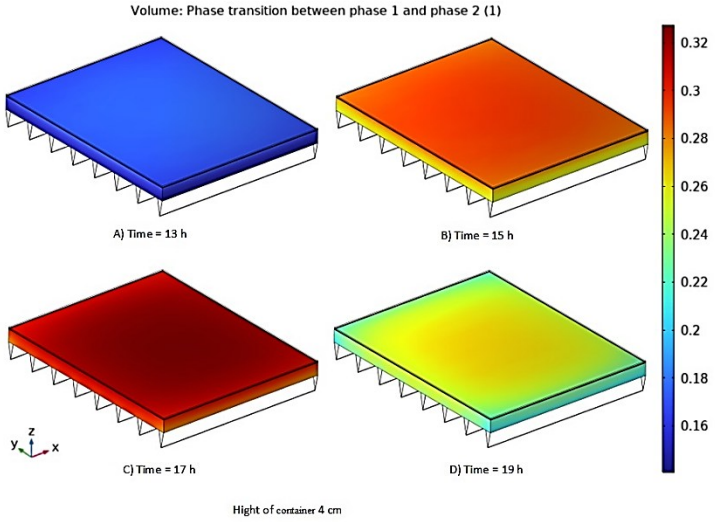

Fig. 12. Contour phase transition between phase solid and phase liquid

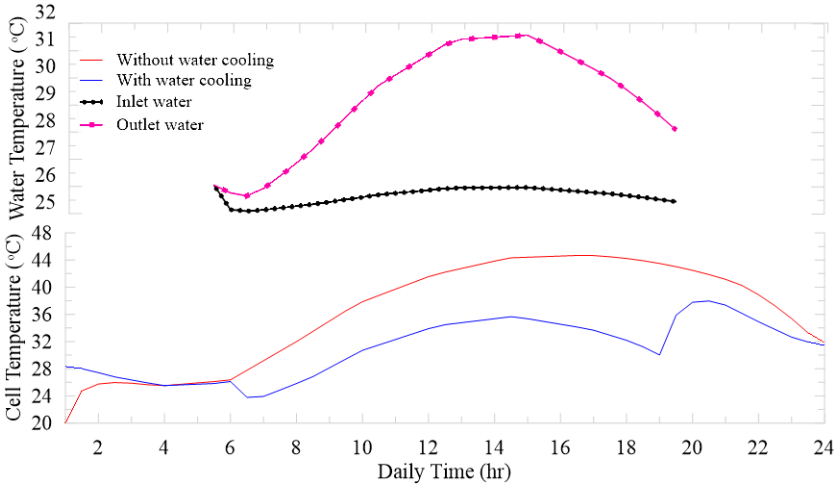

Fig. 13. The effect of cooling water on the PV cell performance

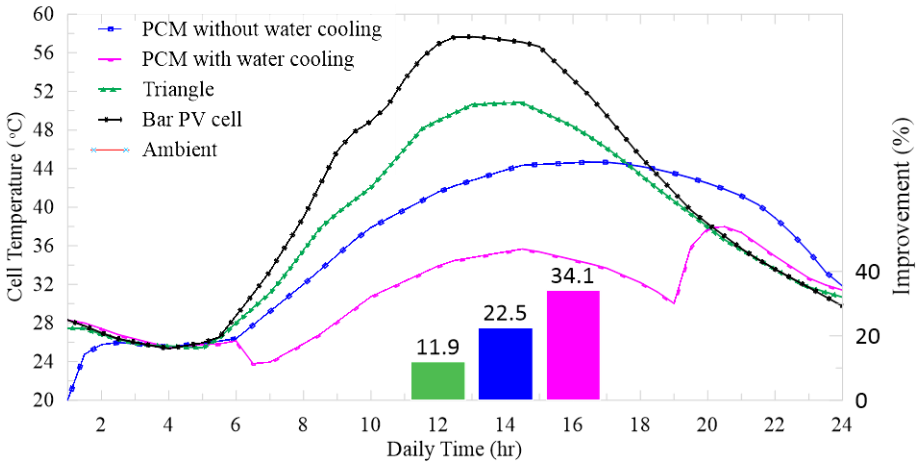

Fig. 14. Comparison of the cooling PV, without affecting the solar panel surface temperature

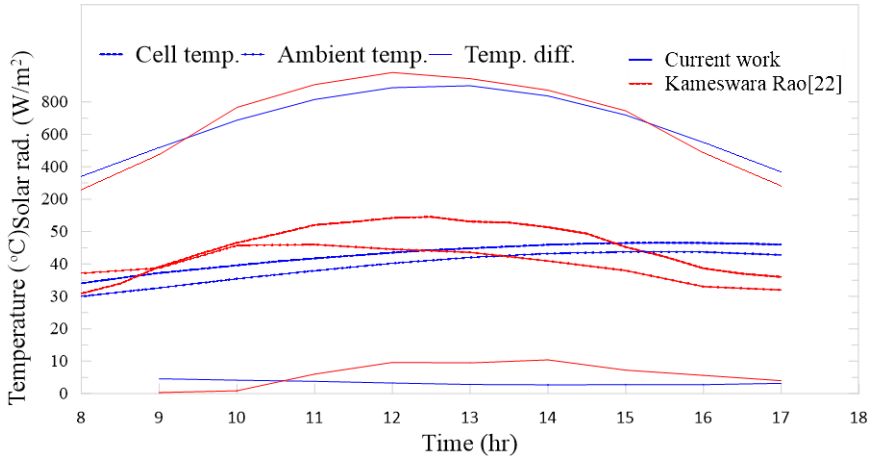

Fig. 15. Comparison between the current work results and D. Kameswara Rao [22] results

4. Conclusions

In this work, several methods were used to reduce the temperature of a 570 x 670 mm PV solar cell. The effect of the number of flat fins was investigated to determine the optimal quantity. Once this was established, the study examined how different fin cross-sections affect cell temperature, eventually identifying the best design. Subsequently, the impact of the nano-PCM mass on cell performance was analyzed. The research concluded with an investigation into how cooling the nano-PCM with water influences results. The results indicated that although the lowest cell temperature was achieved with 10 flat fins, 8 flat fins yielded a temperature similar to that of 10 flat fins. Therefore, the number of fins was fixed at 8, which reduced the cell temperature to 52.6 °C, a 10% improvement. Using triangular-section fins instead of flat ones reduced the maximum temperature to 50.8 °C, which represents an improvement of 11.8%. Furthermore, supporting the heatsink with a 40 mm-thick container filled with nano-PCM reduced the cell temperature to 44.67 °C (a reduction of 22.5%). In this regard, the lowest maximum cell temperature was 37.9 °C when the nano-PCM of the above type was cooled with water, resulting in a 34.1% improvement.

Acknowledgment

The authors gratefully acknowledge the Engineering Technical College–Baghdad, Middle Technical University, Baghdad, Iraq, for providing support and laboratory facilities that significantly contributed to the successful completion of this study.

References

[1] M. Hussein, H. H. Mohammed Ali, and Z. Ali, “Assessing the efficacy of flat-plate solar collectors using nanofluids in the climatic context of Kirkuk city, Iraq”, Acta Polytech, vol. 64, no. 1, pp. 25–33, Mar. 2024, doi: 10.14311/AP.2024.64.0025.

[2] Noor A. Kadhim, Adel A. Obed, Ahmed J. Abid, Ameer L. Saleh, and Reheel J. Hassoon, ‘A Systematic Review for Reconfiguring Photovoltaic Arrays under Conditions of Partial Shading’, Electr. Eng. Tech. J., vol. 1, no. 1 SE-Engineering, pp. 20–34, Jun. 2024, doi: 10.51173/eetj.v1i1.6.

[3] S. A. Hameed, H. H. M. Ali, and S. M. Fakhraldin, “Augmenting the thermal efficiency of solar stills using phase change material on a rotating hollow cylinder,” Int. J. Heat Technol., vol. 43, no. 3, pp. 1187–1194, 2025, doi:10.18280/ijht.430336.

[4] H. Madhi, S. Aljabair, and A. A. Imran, ‘A review of photovoltaic/thermal system cooled using mono and hybrid nanofluids’, Int. J. Thermofluids, vol. 22, p. 100679, 2024, doi: https://doi.org/10.1016/j.ijft.2024.100679.

[5] J. Jiang, Y. Hong, Q. Li, and J. Du, 'Evaluating the impacts of fin structures and fin counts on photovoltaic panels integrated with phase change material', Energy, vol. 283, p. 129143, 2023, doi: https://doi.org/10.1016/j.energy.2023.129143.

[6] Khelifa, M. El Hadi Attia, K. Harby, A. Elnaby Kabeel, M. M. Abdel-Aziz, and M. Abdelgaied, 'Experimental and economic evaluation on the performance improvement of a solar photovoltaic thermal system with skeleton-shaped fins', Appl. Therm. Eng., vol. 248, p. 123180, 2024, doi: https://doi.org/10.1016/j.applthermaleng.2024.123180.

[7] Y. Hong, D. Bai, Y. Huang, and J. Du, 'Effect of T-shaped fin arrangements on the temperature control performance of a phase change material heat sink', Int. Commun. Heat Mass Transf., vol. 148, p. 107073, 2023, doi: https://doi.org/10.1016/j.icheatmasstransfer.2023.107073.

[8] A. Khelifa, M. El Hadi Attia, Z. Driss, and A. Muthu Manokar, 'Performance enhancement of photovoltaic solar collector using fins and bi-fluid: Thermal efficiency study', Sol. Energy, vol. 263, p. 111987, 2023, doi: https://doi.org/10.1016/j.solener.2023.111987.

[9] A. Alqatamin, O. A. Al-Khashman, and J. Su, 'A novel heatsink for optimising photovoltaic cell performance with passive cooling using perforated wave-shaped fins,' J. Sol. Energy Eng., vol. 147, no. 5, p. 051002, 2025, doi:10.1115/1.4068410.

[10] M. A. Bashir and H. M. Ali, 'Numerical investigation of passive cooling of the PV module using extended fin heat sinks: A parametric analysis', Process Saf. Environ. Prot., vol. 195, p. 106749, 2025, doi: https://doi.org/10.1016/j.psep.2025.01.003.

[11] J. Du, D. Bai, X. Meng, F. Jiao, and Y. Hong, 'Effect of Cantor fractal fin arrangements on the thermal performance of a photovoltaic-phase change material system: An experimental study', Int. J. Heat Mass Transf., vol. 219, p. 124853, 2024, doi: https://doi.org/10.1016/j.ijheatmasstransfer.2023.124853.

[12] K. S. Unnikrishnan, K. Santhosh, and B. Rohinikumar, "Experimental and numerical analysis of PV-PCM integrated with novel shaped corrugated fins," *Therm. Sci. Eng. Prog.*, vol. 50, p. 102562, 2024, doi:10.1016/j.tsep.2024.102562.

[13] J. Pu, J. Du, B. Zhang, F. Rong, F. Jiao, and Y. Hong, 'Thermal management enhancement of photovoltaic panels using phase change material heat sinks with various T-shaped fins' , Case Stud. Therm. Eng., vol. 61, p. 104991, 2024, doi:10.1016/j.csite.2024.104991.

[14] M. A. Abdel Salam, M. A. Hassab, W. M. El-Maghlany, and M. A. Alnakeeb, "Assessment of fin configuration effect on the performance of photovoltaic thermal systems with trapezoidal tubes and phase change material," Case Stud. Therm. Eng., vol. 73, p. 106487, 2025, doi:10.1016/j.csite.2025.106487.

[15] S. A. B. Al-Omari, F. Mahmoud, Z. A. Qureshi, and E. Elnajjar, The impact of different fin configurations and design parameters on the performance of a finned PCM heat sink,' Int. J. Thermofluids, vol. 20, p. 100476, 2023, doi:10.1016/j.ijft.2023.100476.

[16] H. Madhi, S. Aljabair, and A. A. Imran, 'Comparative numerical study on the effect of fin orientation on the photovoltaic/thermal (PV/T) system performance,' Int. J. Thermofluids, vol. 24, p. 100909, 2024, doi:10.1016/j.ijft.2024.100909.

[17] T. Ambreen and M. H. Kim, 'Effect of fin shape on the thermal performance of nanofluid-cooled micro pin-fin heat sinks,' Int. J. Heat Mass Transf., vol. 126, pp. 245–256, 2018, doi:10.1016/j.ijheatmasstransfer.2018.05.164.

[18] F. Bayrak, H. F. Oztop, and F. Selimefendigil, "Effects of different fin parameters on temperature and efficiency for cooling of photovoltaic panels under natural convection," *Sol. Energy*, vol. 188, pp. 484–494, 2019, doi:10.1016/j.solener.2019.06.036.

[19] M. S. Ghanim and A. A. Farhan, "Performance evaluation of the photovoltaic thermal system with a fin array and surface zigzag layout," Int. J. Low-Carbon Technol., vol. 17, no. October, pp. 1166–1176, 2022, doi: 10.1093/ijlct/ctac092.

[20] J. Kim and Y. Nam, "Study on the cooling effect of attached fins on PV using CFD simulation," Energies, vol. 12, no. 4, p. 758, 2019, doi:10.3390/en12040758.

[21] J. Mustafa, S. Alqaed, S. M. Sajadi, and H. Aybar, 'Enhancing solar panel cooling efficiency: a study on the influence of nanofluid inclusion and pin fin shape during melting and freezing of phase change materials', Front. Energy Res., vol. 12, no. February, pp. 1–11, 2024, doi: 10.3389/fenrg.2024.1344061.

[22] D. K. Rao, P. Sundaram, K. Selvakumar, D. V. Krishna, A. Sathishkumar, and S. C. Kim, 'Performance assessment of nano-enhanced organic PCM embedded in heat sinks for PV panel thermal management under outdoor conditions', Appl. Therm. Eng., vol. 280, p. 128140, 2025, doi: https://doi.org/10.1016/j.applthermaleng.2025.128140.

[23] H. A. Abdul Kareem, A. Khalifa, and A. Hamad, "Investigation of Photovoltaic Membrane Desalination Utilizing Storage Heat in Solar Cells", International Journal of Thermodynamics, vol. 27, no. 3, pp. 6–14, Sept. 2024, doi: 10.5541/ijot.1390518.

[24] M. Saeed, "Numerical and experimental study enhancement of single-slope solar still productivity using PCM-nanoparticles," M.S. thesis, Al-Furat Al-Awsat Technical University, Iraq, 2019.

[25] Barrak, Anwar S., Nawfal M. Ali, and Hussein H. M. Ali. "An Effect of Binary Fluid on the Thermal Performance of Pulsation Heat Pipe". International Journal of Applied Mechanics and Engineering 27 no. 1 (2022): 21–34. doi:10.2478/ijame-2022-0002.

[26] H. A. A. Kareem, A. J. Hamad, and A. H. N. Khalifa, "Effect of pore membrane size on the cell temperature and water productivity in photovoltaic membrane distillation," AIP Conf. Proc., vol. 3350, no. 1, p. 60017, Nov. 2025, doi: 10.1063/5.0297562.

[27] M. K. Rasheed, H. A. Abdul Kareem, F. A. Kareem, and M. A. Al-Obaidi, "Performance enhancement of solar air heater with different roughness absorber plates," J. Sol. Energy Res., vol. 10, no. 2, pp. 2367–2382, 2025, doi:10.22059/jser.2025.400971.1622.

[28] A. S. Barrak, A. A. M. Saleh, and Z. H. Naji, "A Heat Recovery Device using Oscillating Heat Pipe with Circular and Elliptical Tubes", Int. J. Automot. Mech. Eng., vol. 18, no. 1, pp. 8442 – 8453, Mar. 2021, doi: 10.15282/ijame.18.1.2021.04.0639.

[29] H. Salah, L. Muthana, and R. Al-Zuhairy, "The influence of ambient conditions on compression ignition engine performance: Experimental study," *J. Mech. Eng. Res. Dev.*, vol. 43, pp. 317–325, 2020.